Chapter 2

# INPUT INFORMATION

The MSCE-HM model operation requires various input information among which meteorological parameters, emissions data, land cover information and concentrations of different reactants are the most important. This chapter is devoted to description of these types of the model input data.

## 2.1. Meteorological data

Meteorological data is one of key input parameters when modelling long-range transport and deposition of atmospheric pollutants. Quality of the modelled concentrations and depositions is determined to a large extent by quality of the meteorological data. Modelling of heavy metals requires large set of meteorological parameters. Calculation of advection needs data on wind components at different altitudes of the troposphere. Description of wet removal processes requires data on three-dimensional precipitation rates. Dry deposition parameterisation uses a number of parameters of the atmospheric boundary layer (e.g. friction velocity, Monin-Obukhov length etc.). Most of the parameters are not available from the routine synoptic or aerological observations. Moreover, observation stations are randomly distributed over surface, whereas the modelling needs data on a regular grid. Therefore, it is necessary to use a pre-processing system, which can prepare gridded meteorological parameters with certain temporal resolution.

The MSCE-HM model is meant for utilizing off-line meteorological information. This means that meteorological data are not generated in the process of calculations, but periodically supplied into the model as input data. Therefore, meteorological data have to be prepared in advance and stored in the same model grid as used in the transport model. Direct interpolation of meteorological parameters to the model grid is not a proper way because it can significantly disturb the mass conservation. Besides, some parameters (e.g. atmospheric precipitation) cannot be correctly interpolated in principal. Hence, in order to provide MSCE-HM model with meteorological data a pre-processing system has been developed based on the PSU/NCAR mesoscale model MM5 [*Grell et al*., 1995; http://www.mmm.ucar.edu/mm5/overview.html]. The system utilizes input meteorological data with rough spatial and temporal resolution and performs short-term weather forecast for the transport model grid.

There are several useful features of this system:

- This system can work with different sets of initial meteorological data (NCEP/DOE and ECMWF re-analyses etc.)
- Various parameterisations of physical processes (atmospheric boundary layer, precipitation, radiation transfer etc.) are available.
- This system allows operations in different map projections. In particular, the polar stereographic projection is supported.

- Nesting is available in this system. A user can perform calculations both on regional and local scales on the base of the same data assimilation system.

- The MM5 community model is spread worldwide and tested for various geographical and climatic regions. Besides, the model improvement and development are going on.

- This system can be deployed on a personal computer and can provide simulations of meteorological data for reasonable time.

In the current version of MM5 applied in the pre-processor the atmospheric boundary layer characteristics are parameterized using the *S.-Y.Hong and H.-L.Pan* [1996] scheme. Microphysics of stratiform clouds and precipitation is described according to [*Reisner et al.*, 1998]. The improved Kain-Fritsch scheme [*Kain*, 2002] is used for convective cloudiness parameterization. Besides, the radiation scheme considers interactions of short-wave and long-wave radiation with clouds and cloud-free air and predicts near-surface radiation fluxes. The MM5 forecast domain is larger than the EMEP one by 6 gridcells in each direction to reduce the effects of the lateral boundary conditions.

The following procedure is applied to prepare meteorological data for the transport model. The MM5 reads meteorological data of the objective analysis, interpolates them into EMEP grid performing the four-dimensional data assimilation (FDDA). The aim of FDDA is nudging the forecast to the data of meteorological observations or the objective analysis. Currently we use NCEP/DOE reanalysis data (dataset II) [http://dss.ucar.edu/catalogs/ranges/range090.html] as input information for MM5. More details about the nudging and the FDDA can be found in the MM5 technical documentation [*Grell et al*., 1995]. After the nudging for 6-hours period the meteorological forecast takes place for the further 6-hours. The forecast output is used as input data for the transport model. The pre-processor supplies meteorological parameters with 6-hours temporal resolution. Up to date, meteorological data have been prepared for the period 1990–2003. The set of meteorological data provided by the pre-processor and short description of their usage in the model are summarised in Table 2.1. It should be noted that the vertical component of wind velocity supplied by the pre-processor is not used in the transport model to keep the mass conservation of a pollutant. Instead, the vertical velocity is calculated at each the model timestep from the continuity equation using the procedure described in Chapter 1.

***Table 2.1.*** *Meteorological parameters and their usage in the MSCE-HM model*

| Parameter | Notation | Dimension | Usage |
|---|---|---|---|
| Surface pressure | $p_s$ | 2D | Air density, atmospheric transport |
| Components of wind velocity | $U, V$ | 3D | Atmospheric transport |
| Air temperature | $T_a$ | 3D | Air density, atmospheric chemistry, dry deposition |
| Water vapour mixing ratio | $q_v$ | 3D | Air density, dry deposition |
| Liquid water mixing ratio | $q_w$ | 3D | Atmospheric chemistry, in-cloud scavenging |
| Ice mixing ratio | $q_i$ | 3D | In-cloud scavenging |
| Stratiform precipitation | $R_s$ | 3D | Wet removal |
| Convective precipitation | $R_c$ | 3D | Wet removal |
| Eddy diffusion coefficient | $K_z$ | 3D | Vertical eddy diffusion |
| Monin-Obukhov length * | $L$ | 2D | Stability, dry deposition |
| Surface temperature | $T_s$ | 2D | Natural emission and re-emission |
| Snow cover height | $H_s$ | 2D | Natural emission and re-emission |

* - average over a grid cell

## 2.1. Emission data

Emission data are probably the most important input parameter to a great extent determining results of the modelling. Therefore, reliable values of emission at the model input are vital for realistic pollution levels at the output. Emissions of most heavy metals to the atmosphere include direct anthropogenic component, re-emission of previously deposited mass and emission from natural sources.

### *Anthropogenic emissions*

MSCE-HM model uses for regular calculations gridded anthropogenic emissions data based both on national information officially submitted by the Parties to the Convention and expert estimates. For example, national data on heavy metal emissions for 2002 were submitted by 27 countries. For countries that have not submitted national data, a linear interpolation from previous years or expert estimates [*Berdowski et al.,* 1998; *ESQUAD*, 1994; *Pacyna et al*., 2001] used in the modelling. National information on the spatial distribution of emission sources at least for one year since 1990 was submitted by 18 countries. For the rest of them expert estimates [*Berdowski et al*., 1997] were used to distribute the total national emission over a country.

#### *Emission distribution with height*

Vertical distribution of the pollutant concentration in the vicinity of emission sources as well as long-range atmospheric transport to some extend depend on height of the emission source. For example, emissions from road transport take place near surface, whereas stacks of power stations can be as high as 1-2 hundred meters. Besides, thermal or dynamical effects can lead to significant lifting up the emissions in the atmosphere. In order to estimate distribution of emissions with height we utilized sector-split emission information provided by 20 countries. Height distributions for different emission sectors were averaged taking into account a sector contribution to the total emission. It was assumed that heavy metal emission is distributed between three lowest model layers. The dynamical lifting up of the emitted mass is not currently taken into account. The resulting distribution of lead, cadmium and mercury emissions over three lowest layers is presented in Table 2.2 (based on data for 2000).

***Table 2.2.*** *Heavy metal emission distribution with height*

| Model layer | Layer boundaries (m) | Emission fraction (%) | | |
|---|---|---|---|---|
| | | Pb | Cd | Hg |
| 1 | 0 – 70 | 61 | 40 | 37 |
| 2 | 70 – 150 | 28 | 43 | 38 |
| 3 | 150 – 300 | 11 | 17 | 25 |

#### *Temporal variation*

Anthropogenic emissions of heavy metals have a noticeable temporal cycle (daily, seasonal etc.). Production of heat and, hence, emissions from this sector results in emission increase in winter season. Emissions from road transport sector and from electric power production have minimum at night. Seasonal variation of the emissions is taken into account in the model. The average seasonal

emission amplitudes have been calculated based on multi-years emissions data [*Ryaboshapko et al*., 1999]: 9% with maximum in summer for lead; 8% and 11% with maximum in winter for cadmium and mercury, respectively. It is clear, that emission variations with season can vary not only from country to country, but also in different parts of a big country. However, at present these amplitudes are applied for the whole domain.

## *Physical-chemical forms of heavy metal emissions*

Lead, cadmium and some other heavy metals (nickel, chromium, zinc etc.) and their compounds are characterized by very low volatility. Therefore, it is assumed that they are emitted to the atmosphere in the composition of aerosol particles. In contrast to lead and cadmium, mercury can be emitted both in gaseous and in particulate forms. Besides, gaseous species include elemental and oxidized forms. The speciation of mercury emissions commonly is not included in the information submitted by the Parties to the Convention. Therefore, expert estimates of the mercury emission speciation are used in the model [*Axenfeld et al*., 1991; *Pacyna and Münch*, 1991]. Table 2.3 shows the aggregated data on speciation of mercury emissions in European countries.

***Table 2.3.*** *The ratio of individual mercury forms in direct anthropogenic emissions in various European counties [Axenfeld et al., 1991]*

| Country | Emission fraction (%) | | | Country | Emission fraction (%) | | |
|---|---|---|---|---|---|---|---|
| | $Hg^0$ | $Hg^{II}_{gas}$ | $Hg^{II}_{part}$ | | $Hg^0$ | $Hg^{II}_{gas}$ | $Hg^{II}_{part}$ |
| Albania | 50 | 30 | 20 | Kazakhstan* | 51 | 29 | 20 |
| Armenia* | 51 | 29 | 20 | Latvia* | 51 | 29 | 20 |
| Austria | 58 | 25 | 17 | Lithuania* | 51 | 29 | 20 |
| Azerbaijan* | 51 | 29 | 20 | Luxembourg | 51 | 29 | 20 |
| Belarus* | 51 | 29 | 20 | Netherlands | 36 | 47 | 17 |
| Belgium | 60 | 25 | 15 | Norway | 69 | 23 | 8 |
| Bosnia&Herzegovina* | 56 | 27 | 17 | Poland | 52 | 29 | 19 |
| Bulgaria | 55 | 27 | 18 | Portugal | 63 | 30 | 7 |
| Croatia* | 56 | 27 | 17 | Rep. of Moldova* | 51 | 29 | 20 |
| Cyprus** | 51 | 29 | 20 | Monaco*** | 51 | 30 | 19 |
| Czech Republic* | 52 | 30 | 18 | Romania | 50 | 30 | 20 |
| Denmark | 44 | 40 | 16 | Russia* | 51 | 29 | 20 |
| Estonia* | 51 | 29 | 20 | Serbia and Montenegro * | 56 | 27 | 17 |
| Finland | 74 | 18 | 8 | Slovakia* | 52 | 30 | 18 |
| France | 51 | 30 | 19 | Slovenia* | 56 | 27 | 17 |
| Georgia* | 51 | 29 | 20 | Spain | 64 | 26 | 10 |
| Germany | 60 | 31 | 9 | Sweden | 74 | 19 | 7 |
| Greece | 51 | 29 | 20 | Switzerland | 55 | 27 | 18 |
| Hungary | 52 | 29 | 19 | Macedonia* | 56 | 27 | 17 |
| Island | 100 | 0 | 0 | Turkey** | | | |
| Ireland | 50 | 30 | 20 | Ukraine* | 51 | 29 | 20 |
| Italy | 62 | 29 | 9 | United Kingdom | 52 | 34 | 14 |

* - The speciation is taken based on data for the former USSR, Yugoslavia and Czechoslovakia.

** - The speciation is assumed to be equal to that of Greece.

*** - The speciation is assumed to be equal to that of France

### *Natural emission and re-emission*

Apart from anthropogenic emissions, heavy metals are emitted to the atmosphere from natural sources and due to re-emission of previously deposited substances.

#### *Mercury*

Natural emission and re-emission processes are particularly important for the mercury cycle in the environment. To take into account natural emission of mercury we used global estimates by *C.H.Lamborg et al.* [2002]. According to this work global natural emission of mercury is estimated as much as 1000 t/y from land and 800 t/y from the ocean. Review of mercury natural emission estimates and approaches to parameterization of this process can be found in [*Travnikov and Ryaboshapko*, 2002; *Ilyin et al.*, 2002].

Spatial distribution of natural emission fluxes over land was obtained by scattering the total value throughout the globe depending on mercury content in soils and the surface temperature. From this point of view four surface types were distinguished: (1) glaciers, (2) background soils, (3) soil of the geochemical mercuriferous belts, and (4) soil of mercury deposit areas. No mercury emissions are expected form glaciers. Temperature dependence on mercury emission flux from soil can be described by an Arrhenius type equation. Besides, empirically derived activation energies of the process have close values both for background (17.3-29.4 kcal/mole) and for enriched soils (25.2 kcal/mole) (see Table 2.4). To parameterize the temperature dependence we choose value 20 kcal/mole ($8.37 \cdot 10^4$ J/mole) for all soil types. On the contrary, we consider pre-exponential factor depending on the soil type: the factor for background soil is five times lower than for soils of the mercury belts, and ten times lower than for the deposits areas. Besides, the emission flux is assumed to be zero for negative values of the soil temperature in the centigrade scale. Fitting total land emission in the Northern Hemisphere to the adopted value we obtain the following temperature dependence of the mercury flux from soil (in ng/m$^2$/h):

$$F = \begin{cases} A_s \exp(-E_a / R_{univ} T_s), & T_s > T_0 \\ 0, & T_s \le T_0 \end{cases}, \qquad (2.1)$$

where $E_a$ is the activation energy;

the constant $A_s$ is equal to $3.47 \cdot 10^{14}$ for background soils, $A_s = 1.74 \cdot 10^{15}$ for the mercuriferous belts, and $A_s = 3.47 \cdot 10^{15}$ for deposit areas;

$T_s$ is surface temperature, K;

$T_0 = 273$ K.

***Table 2.4.*** *Activation energy of mercury natural emission from background soils*

| Location | $E_a$ (kcal/mole) | Reference |
|---|---|---|
| Tennessee, USA | 17.3 - 25.8 | *Kim et al*., 1995 |
| Tennessee, USA | 18.0 - 24.9 | *Carpi and Linberg*, 1998 |
| Quebec, Canada | 20.5 | *Poissant and Casimit*, 1998 |
| Michigan, USA | 29.4 | *Zhang et al*., 2001 |

When describing the emission from sea surfaces we accept the idea by *J. Kim and W. Fitzgerald* [1986], who suggested proportionality of mercury emission from the ocean to primary production of organic carbon in seawater. Monthly mean fields of the ocean primary production [*Behrenfeld and Falkowski*, 1997] available through the Internet [http://marine.rutgers.edu/opp/] were used for the parameterization of mercury emission from seawater. The spatial distribution of estimated natural emission of mercury in European region is shown in Fig. 2.1. Rather high emission fluxes are from soils of the geochemical belt in Southern Europe and from coastal seawater with the intensive primary carbon production. The low values of mercury emission over the Mediterranean Sea estimated by this approach are because of low primary productivity in the seawater. These emission fluxes are, probably, underestimated [*Ferrara et al.*, 2000; *Gårdfeldt et al.*, 2003], since there are some biotic or abiotic mechanisms of mercury reduction in seawater not described by the parameterization.

During a period of active usage of mercury in human activity more than one million ton was extracted from the lithosphere, and at least half of that came to the atmosphere [*Travnikov and Ryaboshapko,* 2002]. A great amount of mercury was emitted in the process of coal combustion. *W.F.Fitzgerald and R.P.Mason* [1996] believe that 95% of previously emitted mercury has being accumulated in soil over the globe. Enhanced content of mercury in soils should inevitably lead to its re-emission to the atmosphere.

A tentative approach to assess mercury re-emission from European soils was applied basing on conjunction of the MSCE-HM model with a simple box model [*Ryaboshapko and Ilyin*, 2001]. The transport model calculated mercury depositions accumulated during last century. The box model considered European soils as a single reservoir with two output fluxes – re-emission and hydrological leaching. Mercury lifetime in the box according to re-emission was assumed to be 400 year, and according to the leaching – 950 year. Under accepted assumptions the model predicted that by the end of 20$^{th}$ century total re-emission in Europe could make up 50 t/y. The distribution of mercury re-emission from soil in Europe is illustrated in Fig. 2.2. The most significant re-emission fluxes are in Central Europe in the regions where intensive depositions have been observed for a long time. In some heavy polluted areas (Eastern Germany, for example) the re-emission nowadays can exceed the current direct anthropogenic emission.

More sophisticated parameterization of mercury natural emission and re-emission processes requires further research of mercury behavior in soils and seawater.

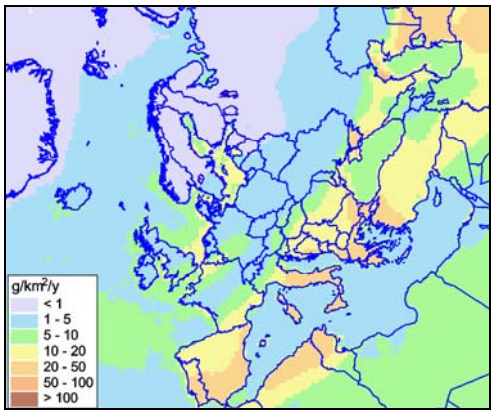


***Fig. 2.1**. Spatial distribution of mercury natural emission in Europe*

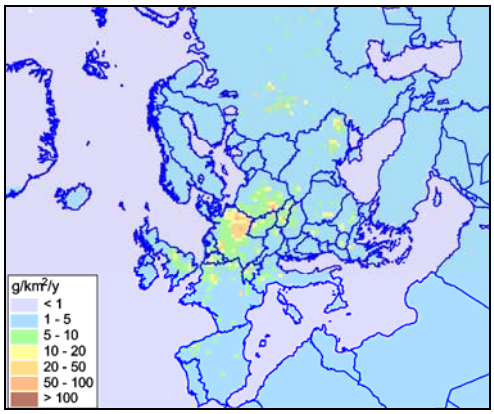


***Fig. 2.2.** Spatial distribution of mercury re-emission from soils in Europe*

*Lead and cadmium*

Lead and cadmium enter the atmosphere not only because of anthropogenic activity, but also due to natural processes. The volcanic activity, sea salt emission, wind re-suspension, wild forest fires and biogenic emissions are suggested as the main processes responsible for natural emission of these metals [*Nriagu*, 1989]. According to *J. Nriagu* [1989], globally averaged flux of lead and cadmium from sea surface is 4 and 0.2 g/km$^2$/y, whereas from land – 54 and 3.7 g/km$^2$/y, respectively. If natural emissions were uniformly distributed over the globe, these fluxes would mean natural emissions within EMEP as much as 900 t/y of lead and 50 t/y of cadmium. These values are much lower than anthropogenic emissions of these metals. However, the available estimates, possibly, do not take into account the accumulation for a long period of heavy metals in the surface layer of European soils. Besides, measurements of heavy metals in seawater indicate significant enrichment (up to orders of magnitude) of the marine surface microlayer with such metals as lead and cadmium especially in polluted regions [e.g. *Weisel et al*., 1984]. Therefore, fluxes of natural emission and re-emission of lead and cadmium in Europe can be significantly higher than globally average ones. A tentative parameterization of lead and cadmium natural emission and re-emission is used in the current version of the model. It is based on measured concentrations of these pollutants in background regions (Atlantic, South Africa, Eastern Asia). The natural emission and re-emission fluxes are assumed to be uniformly distributed over the sea and land surfaces, and evaluated to fit the measured background concentrations. The resulting values of the emission flux for lead and cadmium are 160 and 8 g/km$^2$/y from sea surface and 220 and 12 g/km$^2$/y from soils, respectively. It is also assumed zero emission from surfaces covered with snow.

## 2.3. Land cover

Land cover data is mostly required for evaluation of the dry deposition velocities and assessment of ecosystem-specific depositions. Currently a preliminary land cover dataset developed by the Coordinating Centre for Effects (CCE) is used in the model. The dataset consider 17 landuse/landcover categories listed in Table 2.5 (in the calculations we divide the water surface category into the ocean and inland waters).

***Table 2.5.*** *Land cover categories of CCE dataset used in the model*

| | |
|---|---|
| 1. Temperate coniferous forest | 10. Semi-natural |
| 2. Temperate deciduous forest | 11. Mediterranean scrub |
| 3. Mediterranean needleleaf forest | 12. Wetlands |
| 4. Mediterranean broadleaf forest | 13. Tundra |
| 5. Temperate crops | 14. Desert/Barren |
| 6. Mediterranean crops | 15. Water |
| 7. Root crops | 16. Ice |
| 8. Grasslands | 17. Urban |
| 9. Wheat | |

The dataset is partly based on the database developed in the framework of EC Programme on Coordination of Information on the Environment (CORINE) [dataservice.eea.eu.int]. The information to this database was contributed by European countries. Since the CORINE Land Cover data do not

cover entire EMEP area, Stockholm Environment Institute (SEI) database was used to fill the gaps [http://www.york.ac.uk/inst/sei/APS/projects.html]. In order to unify the CORINE and SEI inventories ecosystem classification EUNIS (European Nature Information System) was adopted.

Parameterization of dry deposition requires some characteristics of the ground surface depending on a landcover category (roughness length, height of vegetation canopy, displacement heights). These characteristics vary from season to season. Five different seasonal categories are considered in the model in accordance with *M.L.Wesely* [1989]:

1. Midsummer with lush vegetation.
2. Autumn with cropland that has not been harvested.
3. Late autumn after frost, no snow.
4. Winter, snow on ground and subfreezing.
5. Transitional spring with partially green short annuals.

Table 2.6 contains the land cover characteristics for the listed above seasons. Roughness length scales for different surfaces and displacement heights are mostly based on [*Brook et al*., 1999]. Roughness length for water surfaces is a function of the friction velocity given by Eq. (1.40) in *Chapter 1*. The heights of vegetation canopy are taken similar to those used in [*Simpson et al*., 2003].

***Table 2.6.*** *Characteristics of different landcover categories used in the model*

| Land cover category | $z_{0m}$ (m) | | | | | *d* (m) | | | | | *H* (m) |
|---|---|---|---|---|---|---|---|---|---|---|---|
| | 1 | 2 | 3 | 4 | 5 | 1 | 2 | 3 | 4 | 5 | |
| Temperate coniferous forest | 0.9 | 0.9 | 0.9 | 0.9 | 0.9 | 15 | 15 | 15 | 15 | 15 | 20 |
| Temperate deciduous forest | 1.05 | 1.05 | 0.95 | 0.55 | 0.75 | 15 | 15 | 7 | 7 | 10 | 20 |
| Mediterranean needleleaf forest | 0.8 | 0.8 | 0.8 | 0.8 | 0.8 | 12 | 12 | 12 | 12 | 12 | 15 |
| Mediterranean broadleaf forest | 1 | 1 | 0.9 | 0.5 | 0.7 | 12 | 12 | 6 | 6 | 8 | 15 |
| Temperate crops | 0.1 | 0.1 | 0.02 | 0.01 | 0.03 | 0.7 | 0.7 | 0 | 0 | 0.3 | 1 |
| Mediterranean crops | 0.2 | 0.2 | 0.04 | 0.02 | 0.06 | 1.5 | 1.5 | 0 | 0 | 0.5 | 2 |
| Root crops | 0.05 | 0.05 | 0.02 | 0.01 | 0.03 | 0.4 | 0.4 | 0 | 0 | 0.2 | 0.5 |
| Semi-natural | 0.05 | 0.05 | 0.03 | 0.01 | 0.03 | 0.4 | 0.4 | 0.2 | 0 | 0.2 | 0.5 |
| Wheat | 0.1 | 0.1 | 0.02 | 0.01 | 0.03 | 0.7 | 0.7 | 0 | 0 | 0.3 | 1 |
| Grasslands | 0.05 | 0.05 | 0.03 | 0.01 | 0.03 | 0.4 | 0.4 | 0.2 | 0 | 0.2 | 0.5 |
| Mediterranean scrub | 0.2 | 0.2 | 0.1 | 0.1 | 0.2 | 2 | 2 | 1 | 1 | 2 | 3 |
| Wetland | 0.05 | 0.05 | 0.03 | 0.01 | 0.03 | 0.4 | 0.4 | 0.2 | 0 | 0.2 | 0.5 |
| Tundra | 0.05 | 0.05 | 0.03 | 0.01 | 0.03 | 0.4 | 0.4 | 0.2 | 0 | 0.2 | 0.5 |
| Desert/Barren | 0.04 | 0.04 | 0.04 | 0.04 | 0.04 | - | - | - | - | - | - |
| Water * | *f*(u*) | *f*(u*) | *f*(u*) | *f*(u*) | *f*(u*) | - | - | - | - | - | - |
| Ice | 0.01 | 0.01 | 0.01 | 0.01 | 0.01 | - | - | - | - | - | - |
| Urban | 1 | 1 | 1 | 1 | 1 | - | - | - | - | - | - |

* - function of the friction velocity (see Eq. (1.40))

## 2.4. Chemical reactants

Atmospheric mercury undergoes chemical transformations both in the gaseous and aqueous phase. Description of the chemical processes involving mercury needs data on spatial and temporal distribution of reactant (ozone, sulfur dioxide, and hydroxyl radical) concentrations in the atmosphere.

Global monthly mean data on $O_3$ and $SO_2$ concentration in the atmosphere calculated by the MOZART model were used. The original data with spatial resolution 2.8°×2.8° were interpolated to the EMEP grid. The obtained spatial distribution of mean annual O3 concentration in the lowest model layer is shown in Fig. 2.3. There is a noticeable gradient of ozone concentration from Northern to Southern Europe. Fig. 2.4 illustrates vertical profiles of ozone concentration in the atmosphere. Each line of the plot demonstrates mean annual ozone concentration averaged along cross-sections shown in Fig. 2.3. According to the figure, ozone concentration increases with altitude in both cases expecting more intensive mercury oxidation by ozone at the upper troposphere.

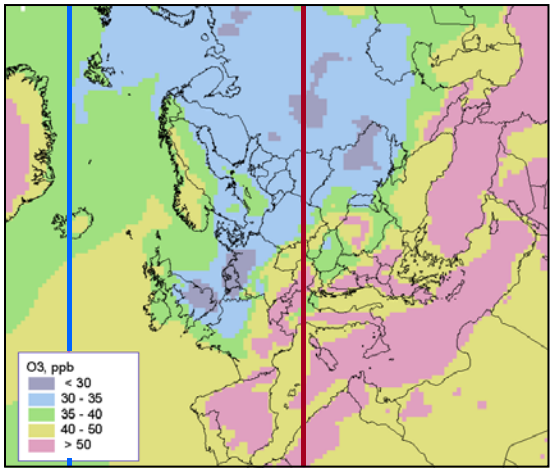


***Fig. 2.3.*** *Spatial distribution of ozone concentration in the ground air of Europe. Lines show cross-sections of the vertical profiles*

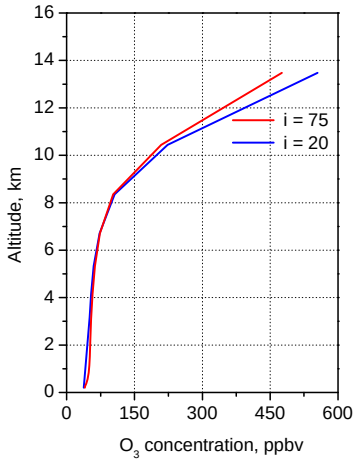


***Fig. 2.4.*** *Vertical profiles of ozone concentration averaged across the model domain*

Fig. 2.5 shows spatial distribution of sulfur dioxide concentration in the surface air of Europe. Spatial pattern of surface concentrations of sulphur dioxide is highly correlated with location of anthropogenic emission sources. Relatively high concentrations are observed in central and western regions of Europe. Relatively low conations are over the Perinea and Scandinavian Peninsulas. As it is shown in Fig. 2.6 the maximum concentrations near the surface and they decrease rapidly with altitude.

For hydroxyl radical in the atmosphere we used modelled monthly mean concentrations from [*Spivakovsky et al.*, 2000]. The original data were interpolated to the EMEP grid. In order to take into account diurnal cycle of OH radical we assume zero concentration at night and concentrations proportional to the cosine of the solar zenith angle during daytime. Besides, air concentrations of OH were decreased by a factor of 10 in the cloud environment and below clouds to account for reduction of its photochemical activity [*Seigneur et al*., 2001].

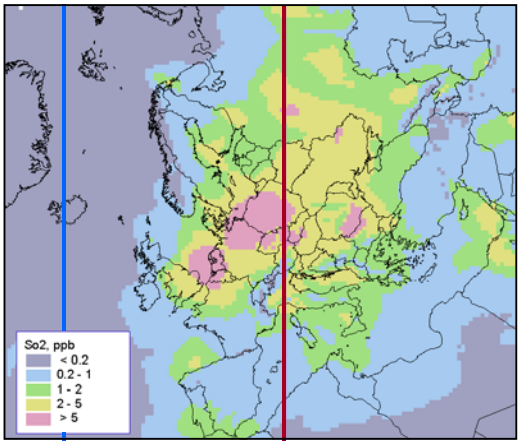


***Fig. 2.5.*** *Spatial distribution of $SO_2$ concentration in the ground air of Europe. Lines show cross-sections of the vertical profiles*

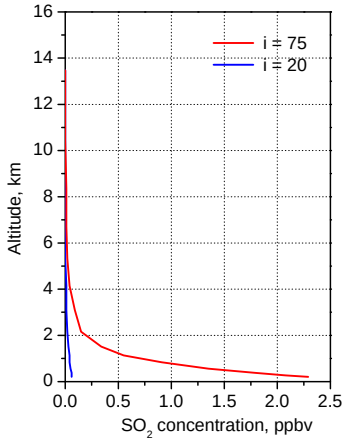


***Fig. 2.6.*** *Vertical profiles of SO2 concentration averaged across the model domain*

Spatial distribution of mean annual hydroxyl radical concentration in the surface air of Europe is shown in Fig. 2.7. The highest concentrations are characteristics of Southern Europe, where surface concentrations where can exceed 0.07 pptv. Vertical distribution of OH radical is characterized by gradual increase with altitude in Atlantic and local maximum the attitude about 2 km in central Europe (Fig. 2.8).

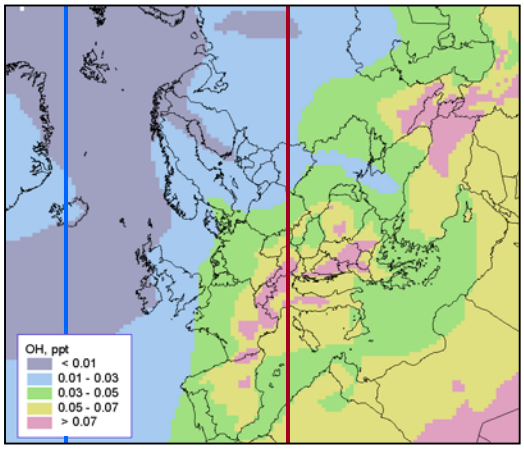


***Fig. 2.7.*** *Spatial distribution of OH radical concentration in the ground air of Europe. Lines show cross-sections of the vertical profiles*

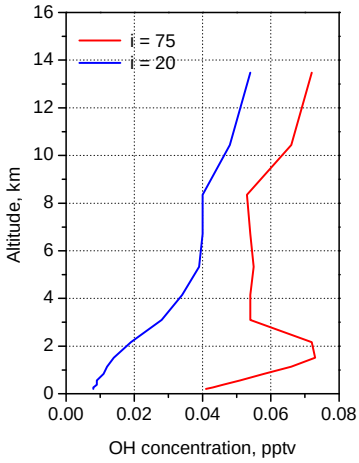


***Fig. 2.8.*** *Vertical profiles of OH radical concentration averaged across the model domain*

The model chemistry also considers oxidation of elemental mercury by chlorine both in gaseous and aqueous phase. To date, the direct production of $Cl_2$ is very poorly characterized. As it is mentioned in [*Keene et al.*, 1999] sea-salt aerosol is the major source of reactive Cl gases (particularly $Cl_2$) in the global troposphere. Following *C.Seigneur et al.* [2001] we adopt air concentration of molecular chlorine in the lowest model layer over the ocean to be 100 ppt at night and 10 ppt during daytime and zero concentration over land. Besides, the model description of aqueous-phase mercury reduction via decomposition of sulphite complexes requires data on cloud water *pH*. In order to obtain monthly mean fields of cloud water *pH* we carried out kriging interpolation of *pH* measurements in precipitation collected within the EMEP monitoring network [*Hjellbrekke*, 2002; http://www.nilu.no/projects/ccc/emepdata.html]. Values of cloud water *pH* over the Atlantic Ocean are set equal to those measured at monitoring site IS02 (Irafoss, Iceland), measurements at site IT01 (Montelibretti, Italy) are taken to characterize the Mediterranean region and Northern Africa.